Pseudophase Separation Model for Surfactant Adsorption: Isomerically Pure Surfactants

4 AUTHORS, INCLUDING:

Jeffrey Harry Harwell

University of Oklahoma

177 PUBLICATIONS   **5,183** CITATIONS

Pseudophase Separation Model for Surfactant Adsorption: Isomerically Pure Surfactants[†]

Jeffrey H. Harwell

School of Chemical Engineering and Materials Science, University of Oklahoma, Norman, Oklahoma 73019

Josiah C. Hoskins and Robert S. Schechter*

Department of Chemical Engineering, University of Texas at Austin, Austin, Texas 78712

William H. Wade

Department of Chemistry, University of Texas at Austin, Austin, Texas 78712

A new model of surfactant adsorption is presented which incorporates the contributions of the hydrophobic effect, surfactant surface aggregation, surface heterogeneities, and counterion concentrations. The basic assumptions of the new model are that surfactant aggregates forming at the solid/solution interface form locally on the surface because of surface heterogeneity and that these local aggregates, which are pictured as bilayered and are called admicelles, can be treated as a pseudophase, an approach that has been applied successfully to the phenomenon of micelle formation, though with well-known and acknowledged limitations. Development of the model includes a rather detailed treatment of the electrostatics of adsorbed surfactant aggregates including so-called discreteness of charge effects. After development of a detailed model, a simplified model is applied to experimental data. It is shown that the adjustable parameters assume physically acceptable values which in turn indicates that the estimated molecular parameters, characteristic of the molecular structure of the surfactant, represent reasonable values. The resulting cumulative distribution of the surface charge density in effect characterizes the surface at a certain temperature, pH, and added electrolyte.

Introduction

The physical adsorption of surfactant from aqueous solution is a phenomenon of central importance in applications ranging from ore flotation and paint technology to enhanced oil recovery. It is also a process of considerable complexity and scientific interest. This interest stems primarily from the propensity of adsorbed surfactant molecules to interact with one another giving rise to surface aggregates which appear to form as a result of a two-dimensional phase transition.[1-5] The mechanism driving formation of the surface aggregates is precisely the same one that causes the formation of micelles in aqueous solution—the hydrophobic effect.[6,7]

A second factor determining surfactant adsorption is the surface charge,[4,8,9] which is known to be a function of the solution pH for ionogenic surfaces.[10-14] The charge on the surface is due to protonation or deprotonation of chemically adsorbed water molecules. Detailed mechanisms for surface amphoteric groups, called the surface site model, have gained widespread acceptance[15,16] and application.[17]

Another feature of surfactant adsorption that is of primary importance is the role of surface heterogeneities. The shape of the isotherm is in fact sensitively related to the distribution of adsorption energies.[2,5,18]

A satisfactory theory for surfactant adsorption must necessarily incorporate these three mechanisms: the hydrophobic effect, surface aggregation of adsorbed molecules, and surface heterogeneities. Scamehorn, Wade, and Schechter[5] have published a theory that satisfies these minimum requirements. Their work demonstrates the importance of the hydrophobic effect even in the region for which surface coverage is sparse and shows that it is

the driving force for the formation of surface aggregates. The aggregates result from a two-dimensional phase transition and tend to be bilayers, much like lipid membranes, when charged surfactants adsorb from aqueous solution on oppositely charged surfaces. Scamehorn et al.[5] allowed for the possibility of first-layer phase transitions to occur with subsequent adsorption of surfactant on top of the first layer to complete the bilayered structure. Calculations, however, showed that very little of the surface was ever covered by a monolayer. As the monolayer formed patchwise on the surface, the second layer tended to form almost simultaneously on top of the first. Thus, the surface was essentially covered by either bilayered structures or by sparsely adsorbed molecules depending on the energy of the particular surface patch. High-energy

(1) Cases, J. M.; Mutaftschiev, B. *Surf. Sci.* 1968, *9*, 57–72.
(2) Cases, J. M. *Bull. Mineral.* 1978, *102*, 684.
(3) Gatta, G. D.; Fubini, B.; Sradella, L. *J. Chem. Soc., Faraday Trans. 2* 1977, *73* (8), 1040.
(4) Gaudin, A. M.; Fuerstenau, D. W. *Min. Eng.* 1955, *7*, 66.
(5) Scamehorn, J. F.; Schechter, R. S.; Wade, W. H. *J. Colloid Interface Sci.* 1982, *85*, 463.
(6) Ben Naim, A. "Hydrophobic Interactions"; Plenum: New York, 1980.
(7) Shinoda, K. *Bull. Chem. Soc. Jpn.* 1953, *26*, 101.
(8) Somasundran, P.; Fuerstenau, D. W. *J. Phys. Chem.* 1966, *70*, 90.
(9) Wakamatsu, T.; Fuerstenau, D. W. *Adv. Chem. Ser.* 1968, *79*, 161.
(10) Davis, J. A.; James, R. O.; Leckie, J. O. *J. Colloid Interface Sci.* 1978, *63*, 480.
(11) Holm, L. W. 57th Annual Fall Technical Conference and Exhibition of the Society of Petroleum Engineers, New Orleans, LA, Sept 26–29, 1982; SPE 11196.
(12) Trogus, F.; Schechter, R. S.; Wade, W. H. *J. Colloid Interface Sci.* 1979, *70*, 293.
(13) Wade, W. H.; Hackerman, N. *J. Phys. Chem.* 1960, *64*, 1196.
(14) Yates, D. E.; Levine, S.; Healy, T. W. *Trans. Faraday Soc.* 1974, *70*, 1807.
(15) Anderson, M.; Bauer, C.; Hansmann, D.; Loux, N.; Stanforth, R. *Adsorpt. Inorg. Solid-Liq. Interfaces* 1981, 1.
(16) James, R. O.; Parks, G. A. *Surface Colloid Sci.* 1982, 12.
(17) Riese, A. C. Doctoral Dissertation, Colorado School of Mines, Golden, 1982.
(18) Cases, J. M.; Goujon, G.; Smani, S. *AIChE Symp. Ser.* 1975, *No. 71*, 100.

patches are, therefore, covered by bilayers at low surfactant solution concentration with the bilayer coverage extending to successively lower energy patches as the solution concentration increases.

The purpose of this paper is to present a new theory of surfactant adsorption. Since the work of Scamehorn et al.[5] does consider the three essential mechanisms governing surfactant adsorption, it might be appropriate to wonder why a new theoretical approach is needed. The present goal is to achieve a unified theory that not only takes into account the important mechanisms of adsorption but also is coupled to modern theories describing ionogenic surfaces (for example, the site binding model) and that includes consideration of the counterions, both their concentration and their specific structure. Such a unified theory should also predict the net surface charge as a function of counterion concentration, pH, and the surfactant concentration so that ζ-potential measurements can be used to help confirm proposed mechanisms of adsorption. The theory proposed by Scamehorn et al.[5] depends on adjustable parameters to describe the adsorption at different values of pH and counterion concentration and type since the role of these is not explicitly included in their treatment. A unified theory should also address the role of surfactant structure for which the theory presented here provides a framework.

To accomplish these far reaching goals, we shall sacrifice some of the thermodynamic precision of the previous work. Our approach can be likened to using the pseudophase separation model for micellization.[19] This model has proven to be one of enormous utility even though it is well-known that it is thermodynamically imprecise. To describe aggregates containing small number of molecules, a mass action approach is required. Despite the thermodynamic weakness of the pseudophase separation model, it has been successfully applied to demonstrate the effects of electrolyte, surfactant structure, surfactant mixtures, and cosolvents on the critical micelle concentration (CMC). These matters are difficult to consider in the context of the mass action model.

The approach considered here is a pseudophase separation model for surfactant adsorption. It assumes that when surfactants having a charge opposite to that of the surface adsorb, the aggregates that form are bilayers. Monolayers do not form. These bilayered structures are called admicelles (adsorbed micelles), and, because they are complete micelles, we distinguish them from "hemimicelles" (or half-micelles), a term used previously in the literature.[3,4] Since hemimicelles do form in some cases,[20] it is necessary to distinguish them from the bilayered structures considered here.

The Admicelle: A Pseudophase

Simply expressed, the admicelle hypothesis maintains that surfactant aggregation producing a bilayered structure (admicelle) occurs on a given patch of a heterogeneous surface at a critical solution concentration (CAC, critical admicelle concentration) which is specific for that patch and for concentrations less than the patch CAC; surfactants adsorbed on that patch do not interact with one another. This hypothesis implies that if the surface is homogeneous, an adsorption isotherm will consist of a

low-concentration region, region I, in which the adsorption will increase slowly with concentration and a vertical step to complete bilayer coverage at the CAC. Adsorption will then remain constant at increased solution concentrations because bilayer coverage represents complete saturation of the surface. If, instead, the surface is made up of a distribution of patches with different adsorption energies, the overall isotherm will appear as a series of step changes in surfactant adsorption.[5] Isotherms having this characteristic shape have been reported.[21]

In this study, the surface charge density, σ_S, is the important characteristic of a surface patch which determines the CAC of the patch. Thus, for each solution of given surfactant concentration and counterion concentration, there corresponds a surface charge density sufficient to stabilize an admicelle; the assumption here is that all patches with this charge density will be covered with surfactant bilayers. Those with lower charge densities will have surfactants adsorbing independently of one another. The total adsorption of surfactant at a given surfactant and counterion concentration is therefore given by the sum of two contributions as follows:

$$\Gamma_{S^-} = \Gamma_{\text{bilayer}} \int_{\sigma_S^*}^{(\sigma_S)_{\text{max}}} f(\sigma_S) \, d\sigma_S + \int_{(\sigma_S)_{\text{min}}}^{\sigma_S^*} f(\sigma_S) \Gamma_I(\rho_{S^-}, \rho_{Na^+}, \sigma_S) \, d\sigma_S \quad (1)$$

where Γ_{S^-} is the Gibb's adsorption, Γ_{bilayer} is the bilayer adsorption density, σ_S^* is the charge density on the mineral oxide surface below the admicelle that just formed at the solution monomer and counterion concentration, $(\sigma_S)_{\text{max}}$ and $(\sigma_S)_{\text{min}}$ are the minimum and maximum charge densities on the mineral oxide, $\Gamma_I(\rho_{S^-}, \rho_{Na^+}, \sigma_S)$ is an isotherm appropriate for low surface coverages, such as the Stern–Grahame–Gouy equation, the site binding model,[14] or, for small variations of salt concentration at high total electrolyte concentration, a Henry's law model, ρ_S and ρ_{Na} are the bulk concentrations of surfactant and counterion, respectively, and $f(\sigma_S)$ is the distribution function for the surface charge. The distribution function is defined so that $f(\sigma_S) \, d\sigma_S$ is the fraction of the surface having a charge density between σ_S and $\sigma_S + d\sigma_S$. Introducing the cumulative distribution function $F(\sigma_S)$, where $F(\sigma_S)$ is the fraction of the surface having a charge density greater than or equal to σ_S, and assuming Henry's law to be an adequate approximation for region I adsorption, we obtain

$$\Gamma_{S^-} = \Gamma_{\text{bilayer}} F(\sigma_S^*) + H\rho_{S^-}[1 - F(\sigma_S^*)] \quad (2)$$

Equations 1 and 2 are deceptively simple. To solve for σ_S at given surfactant and salt concentrations requires not only an expression for the surface distribution functions, $F(\sigma_S)$, but also an expression for the surfactant and salt concentration as a function of surface charge density at which an admicelle will form. Derivation of this latter expression will take up the next sections of this paper.

Chemical Equilibria

Ben Naim[22] has obtained, using statistical mechanical arguments, the chemical potential of a solute molecule in a mixture as follows:

$$\mu_i = W(i|\{\rho_j\}) + kT \ln (\rho_i \Lambda_i^3 q_i^{-1}) \quad (3)$$

where $W(i|\{\rho_i\})$ is the work of putting a molecule of type

(19) Fowler, R. H.; Guggenheim, E. A. "Statistical Thermodynamics"; Cambridge Press: Cambridge, 1939; Chapter 12.

(20) Aston, J. T.; Furlong, D. N.; Grieser, F.; Scales, P. J.; Warr, G. G. In "Adsorption at the Gas–Solid and Liquid–Solid Interface"; Rouquerol, J., Sing, K. S. W., Eds.; Elsevier Scientific Publishing Co.: Amsterdam, 1982.

(21) Casas, J. M.; Canet, D.; Doerler, N.; Poirier, J. E. In "Adsorption at the Gas–Solid and Liquid–Solid Interface"; Rouquerol, J., Sing, K. S. W., Eds.; Elsevier Scientific Publishing Co.: Amsterdam, 1982.

(22) Ben Naim, Arieh "Water and Aqueous Solutions"; Plenum: New York, 1974.

i at a fixed position within the bulk. This work is dependent upon the number densities of the components in the bulk, $\{\rho_j\} \equiv \{\rho_w, \rho_2, ..., \rho_m\}$. The internal partition function for *i* is q_i (assumed independent of the local environment), and the translational contributions are defined by

$$\Lambda_i = \left(\frac{h}{2\pi m_i kT}\right)^{1/2} \qquad (4)$$

A similar analysis for a layered two-dimensional system treated as a separate phase can be carried out to determine the chemical potential of a molecule in the admicelle phase.[23] Thus,

$$\mu_i = \bar{W}(i\|\{\Gamma_j\}) + kT \ln (4\pi^2 \Gamma_i \Lambda_i^2 \bar{q}_i^{-1}) \qquad (5)$$

where $\bar{W}(i\|\{\Gamma_j\})$ is the work of placing a molecule *i* at a fixed position within the admicelle in its most favorable orientation. The composition of the admicelle is given by the set of adsorption densities of the various species in the admicelle, $\{\Gamma_j\}$. Equations 3 and 5, while they are similar in appearance, differ. The Γ_i is the surface densities of *i* whereas the ρ_i is bulk concentrations. The forms of eq 3 and 5 thus reflect the dependence of the two work terms on the composition of the respective systems. The term $4\pi^2$ arises in eq 5 from loss of orientational degrees of freedom of an asymmetric molecule on adsorption[23] into an admicelle. For spherically symmetric counterions, there is no loss of orientational degrees of freedom on adsorption, and the term $4\pi^2$ should be deleted from eq 5 and 6.

At equilibrium, we require the chemical potentials to be equal and for surfactant molecules in an admicelle this becomes

$$\frac{(\bar{W}_i - W_i)}{kT} + \ln\left(\frac{4\pi^2 \Gamma_i}{\bar{q}_i} \frac{q_i}{\rho_i \Lambda_i}\right) = 0 \qquad (6)$$

When only a single type of surfactant molecule is present in the aggregates, that is, for pure component adsorption, $\rho_i = \rho_S$ is the critical admicelle concentration (CAC) of the local patch on which the admicelle has formed.

When a surfactant monomer adsorbs directly in the Stern plane in region I type adsorption rather than in an admicelle, the orientation restrictions are somewhat different and the following expressions result:

$$\mu_i = \bar{W}(i\|\{\Gamma_j\}) + kT \ln (2\pi \Gamma_i \Lambda_i^2 \bar{q}_i^{-1}) \qquad (7)$$

and

$$\frac{(\bar{W}_i - W_i)}{kT} + \ln\left(\frac{2\pi \Gamma_i}{\bar{q}_i} \frac{q_i}{\rho_i \Lambda_i}\right) = 0 \qquad (8)$$

Equation 6 can be compared to the expressions derived by Shinoda for micelles,[7] using Fowler and Guggenheim's "crude yet useful model" of the chemical potential of a molecule in dilute solution.[19]

The next task is an analysis of the work required to transfer a surfactant molecule from the bulk to the interface, $(\bar{W}_i - W_i)$, either to the Stern plane for surfactants adsorbing in region I type adsorption on a local patch or into an admicelle for surfactants or counterions being incorporated into that structure. We will assume here, following Shinoda's[7] treatment of micelles, that the two most significant contributions to the work term are the head/head Coulombic interactions and the tail/tail hy-

drophobic interactions. For region I adsorption, Coulombic and tail/surface interactions are assumed to be of first-order importance. There are, of course, a number of second-order effects of varying, and usually unknown, magnitude. Among those included in various attempts at modeling either micelles or arbitrary charged interfaces are the so-called image potentials,[26-29,46] the entropy change on removing a simple ion from aqueous solution,[29-31] the change in charge density with addition of a new ion,[32] and the work of expanding the micelle/aqueous solution "interface" due to the "interfacial tension".[33] Many of these are claimed by the authors cited to be significant, while other authors among those mentioned ignore them or state them to be insignificant. When one begins to include second-order effects in a model, it is often necessary to deal with all known second-order effects simultaneously, as they may be found to cancel out to a large extent (see, for example, Outhwaite et al.[34] for a study of correction terms to be Poisson–Boltzmann equation). In the study presented here, all of these effects will be neglected; refinements in the model way well require their inclusion. To the first approximation, the work term is given by the expression

$$(\bar{W}_i - W_i) = E^{\text{el}} - m\bar{\omega}_A \qquad (9)$$

Where E^{el} is the electrical work and $m\bar{\omega}_A$ the free energy change on removing the hydrocarbon moiety from aqueous solution to the admicelle, *m* being the number of methyl groups and $\bar{\omega}_A$ the free energy change per methyl group.[24] For counterions adsorbing into the charged regions of the admicelle or into the Stern plane of the surface in region I, the corresponding expression is

$$(\bar{W}_i - W_i) = E^{\text{el}} \qquad (10)$$

(23) Harwell, J. F. Ph.D. Dissertation, The University of Texas at Austin, 1980.
(24) Scamehorn, J. F. Ph.D. Dissertation, The University of Texas at Austin, 1980.
(25) Fernandez, M.S. Thesis, The University of Texas at Austin, 1978.

(26) Buff, F. P.; Goel, N. S. *J. Chem. Phys.* **1969**, *51*, 4983; *J. Chem. Phys.* **1969**, *51*, 5363; *J. Chem. Phys.* **1972**, *56*, 4245.
(27) Buff, F. R.; Goel, N. S. *J. Chem. Phys.* **1972**, *56*, 2405.
(28) Levine, S.; Robinson, K.; Bell, G. M.; Mingins, J. *Electroanal. Chem.* **1972**, *38*, 253; *Electroanal. Chem. Interface Electrochem.* **1973**, *41*, 159; *Electroanal. Chem. Interface Electrochemistry* **1973**, *47*, 395.
(29) Bockris, J. O'M.; Devanathan, M. A. V.; Muller, K. "On the Structure of Charged Interfaces"; Royal Society: London, 1962.
(30) Mukerjee, P. *J. Phys. Chem.* **1962**, *66*, 943.
(31) Mukerjee, P. *J. Phys. Chem.* **1969**, *73*, 2054.
(32) Stigter, D. "Micelle Formation by Ionic Surfactants" I. Two Phase Model, Gouy-Chapman Model, Hydrophobic Interaction, *J. Colloid Interface Sci.* **1974**, *47*, 2; *J. Phys. Chem.* **1974**, *78*, 2480; *J. Phys. Chem.* **1975**, *79*, 1008; *J. Phys. Chem.* **1975**, *79*, 1015.
(33) Jonnson; Bengt; Wennerstrom, H. *J. Colloid Interface Sci.* **1981**, *80*, 482.
(34) Outhwaite, C. V.; Bhuiyan, L. B.; Levine, S. *J. Chem. Soc., Faraday Trans. 2* **1980**, *76*, 1388.
(35) Levine, S.; Bell, G. M.; Calvert, D. *Can. J. Chem.* **1962**, *40*, 518.
(36) Levine, S.; Mingins, J.; Bell, G. M. *J. Electroanal. Chem.* **1967**, *13*, 280–329.
(37) Maxwell, J. C. "A Treatise on Electricity and Magnetism", 3rd ed.; Dover: New York, 1954; Vol. I. Originally published by Clarendon Press in 1891.
(38) Jackson, J. D. "Classical Electrodynamics", 2nd ed.; Wiley: New York, 1975.
(39) Booth, F. *J. Chem. Phys.* **1951**, *19*, 391.
(40) Churchill, R. V. "Operational Mathematics"; McGraw-Hill: New York, 1972; Chapter 15.
(41) Bockris, J. O'M.; Reddy, A. K. N. "Modern Electrochemistry"; Plenum/Rosetta: New York, 1977; Vol. I.
(42) Lindeman, B.; Wennerstrom, H. *Top. Curr. Chem.* **1980**,
(43) Hirasaki, G. J.; Lawson, J. B. 57th Annual Fall Technical Conference and Exhibition of the Society of Petroleum Engineers of AIME, New Orleans, LA, Sept 26–29, 1982; SPE 10921.
(44) Morterra, C.; Ghiotti, G.; Garrone, E.; Boccuzzi, F. *J. Chem. Soc. Faraday Trans. 1* **1976**, *72*, 2722.
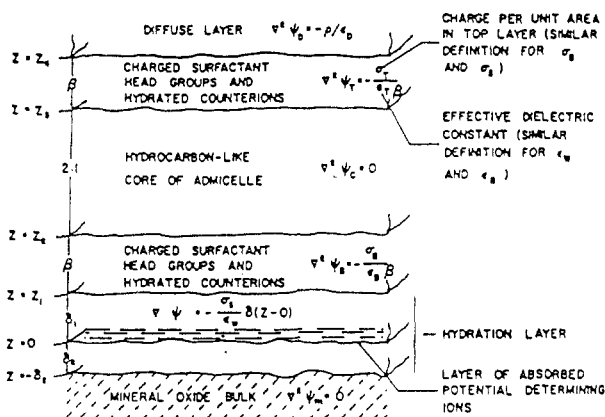(45) Nunn, C. C. Ph.D. Dissertation, The University of Texas at Austin, 1981.
(46) Bockris, J. O.'M.; Habib, M. A. *J. Res. Inst. Catal., Hokkaido Univ.* **1975**, *23*, 47.

Figure 1. Model used to describe the electrostatic field in an admicelle.

where all other terms will be neglected. For a monomer adsorbing at the inner Helmholtz plane (IHP) in region I, it is assumed that the work term is given by

$$(\bar{W}_i - W_i) = E^{\text{el}} - n\bar{\omega}_i \qquad (11)$$

where n, the effective number of methyl groups removed from solution to the IHP, may not be equal to m, the effective number of groups removed to the admicelle. We also expect that the $\bar{\omega}_A \neq \bar{\omega}_I$. There will be no further attempt at analysis of the terms for the hydrophobic effect; $\bar{\omega}_A$, $\bar{\omega}_I$, m, and n will be treated as adjustable parameters.

Electrostatics of Surfactant Adsorption

Evaluation of the CAC for a local patch from eq 6 requires an expression for the electrical potential of a surfactant ion in an admicelle relative to the bulk. Similarly, evaluation of the Henry's law coefficient for a local patch requires the electrical potential of a monomer on the surface relative to the bulk. In this section, approximations will be presented for these quantities based on the equations of classical electrostatics. The analysis begins with the electrostatic fields in an admicelle. The procedure will be as follows:

(1) Find the potential for placing an infinitesimal test charge in the admicelle. In this derivation, the charge of the admicelle head will be smeared out uniformly though the region of the admicelle containing the charged surfactant head groups and adsorbed counterions (see Figure 1).

(2) Correct this potential (to be referred to as the macropotential) for the finite size of the ions and the discreteness of the charge. Real ions are not of negligible size relative to the size of the admicelle, and assuming a smeared out charge distribution up to the center of the ion will overestimate the potential. Real charge carriers have a distance of closest approach. Hence, the potential actually experienced by the ion, called here the micropotential, will be corrected from the macropotential by excluding the smeared out charge distribution from a sphere about the ion and its nearest neighbors in the admicelle.

(3) The contribution of nearest-neighbor interactions to the micropotential will be estimated by assuming a local structure about the ion and evaluating Coulombic interactions between the ion of interest and its neighbors.

The equations describing the macropotential (the potential of an infinitesimal test charge), the assumed structure of the admicelle, and definitions of the parameters in the equations are found in Figure 1. Note that σ_T, for example, is the net charge in the upper layer of the admicelle obtained from adding together the charges on

the surfactant ions and the charges on the adsorbed counterions. The term σ_T has units of charges/nm^2, but σ_T/β has units of charges/nm^3. Thus, the equation giving the Laplacian of the potential in the upper layer assumes the net charge in that layer has been smeared out uniformly throughout the layer.

Integration of the equations shown in Figure 1 produces the following expressions for the potential in the diffuse layer, within the top and bottom layers and at the surface:

$$\psi_D\big|_{z=z_4} \equiv \psi_D{}^* = \frac{kT}{e}\cosh^{-1}\left\{1 + \frac{\sigma_0{}^2}{4kT\rho_0\epsilon_D}\right\} \qquad (12)$$

$$\psi_T(z) = -\frac{\sigma_T}{2\epsilon_T\beta}z^2 + A_Tz + B_T, \quad z_3 \le z \le z_4 \qquad (13)$$

$$\psi_B(z) = -\frac{\sigma_B}{2\epsilon_B\beta}z^2 + A_Bz + B_B, \quad z_1 \le z \le z_2 \qquad (14)$$

$$\psi_W(z) = \psi_W|_{-\epsilon} + \frac{d\psi}{dz}\big|_{-\epsilon}(z + \epsilon) - \frac{\sigma_S}{\epsilon_W}zU(z), \quad -\delta_2 \le z \le z_i \qquad (15)$$

$$\psi_M(z) = A_Mz + B_M, \quad z \le -\delta_2 \qquad (16)$$

where σ_T is the net charge density of the upper charge layer of the admicelle in units of charges/nm^2, σ_B is the analogous quantity for the lower region of the admicelle, σ_S is the charge in the hydration layer of the mineral oxide, σ_0 is given by $\sigma_0 = \sigma_B + \sigma_T + \sigma_S$, and ϵ_T, ϵ_B, ϵ_W, ϵ_D, and ϵ_M are the effective dielectric constants in the appropriate regions. The solution ion concentration is $\rho_0 = \rho_{S^-} + \rho_{Na^+}$. The expression $U(z)$ is the Heaviside function.

From Gauss's law, the condition of electroneutrality, and the boundary conditions we obtain the constants of integration

$$A_T = \frac{\sigma_T z_4}{\epsilon_T\beta} - \frac{\sigma_0}{\epsilon_T} \qquad (17)$$

$$B_T = \psi_D{}^* - \frac{\sigma_T z_4{}^2}{2\epsilon_T\beta} + \frac{\sigma_0 z_4}{\epsilon_T} \qquad (18)$$

$$A_B = \frac{\sigma_B z_1}{\epsilon_B\beta} - \frac{\sigma_S}{\epsilon_B} \qquad (19)$$

$$B_B = \frac{\sigma_B z_2{}^2}{2\epsilon_T\beta} - \frac{\sigma_B z_1 z_2}{\epsilon_B\beta} + \frac{\sigma_S z_2}{\epsilon_B} - \frac{(\sigma_B + \sigma_S)}{\epsilon_C}z_2 + \psi_D{}^* + \frac{\sigma_0\beta}{\epsilon_T} + \frac{\sigma_B + \sigma_S}{\epsilon_C}z_3 - \frac{\sigma_T z_3{}^2}{2\epsilon_T\beta} \qquad (20)$$

$$B_M = \psi_W|_{-\epsilon} = B_B + \frac{\sigma_B z_1{}^2}{2\epsilon_B\beta} + \sigma_S z_1\left(\frac{1}{\epsilon_W} - \frac{1}{\epsilon_B}\right) \qquad (21)$$

Equations 12–16 give the macropotential inside the charged layers of the admicelle in terms of σ_B, σ_T, and σ_S, the smeared out net charge densities. This is not the potential experienced by the surfactant ion or an adsorbed counterion. (Compare Levine et al.[28,35,36] and Buff and Goel.[27]) One reason already mentioned is the finite size of the charge carriers and the discreteness of the charge; real ions have a distance of closest approach and integer charge. We will correct for the first effect by excluding the smeared out charge from a sphere about the ion of interest that includes the central ion and its nearest neighbors. The second reason the macropotential does not describe the potential actually experienced by the real ion is that Maxwell's equations, which include the Poisson and

Laplace equations used to arrive at eq 13–16, give the field experienced by an infinitesimal test charge; for example, they assume the charge on the test particle is negligible. As a result, there is no correlation between the position of the test charge and the positions of the other charge carriers. Again, the real ion does not fit this description either. Because it carries a finite charge, oppositely charged ions are most likely to be its nearest neighbors; i.e., at least locally there is a correlation between the position of the ion and the position of other ions in the system. This effect will be introduced in an ad hoc manner later in the development. The finite charge of the ion also causes the molecules in the surrounding media to orient themselves relative to the ion of interest; as they are partially oriented in response to the ion's charge, an induced field is set up which modifies the potential experienced by the ion. This self-induced change in the local value of the field is often called the self-image potential, imaging, or the image effect, not because the charge interacts with an induced image, but because the change in the field can be found exactly by the method of images in systems of relatively simple geometry without solving the Poisson and Laplace equations explicitly (Maxwell, ref 37, Chapter XI). The combination of these various corrections to the macropotential for the finite size and charge of the ion are often referred to as discreteness-of-charge effects.[28]

We begin to account for these effects by replacing the real ion by a point charge at the center of a sphere (Jackson, ref 38, Chapter 4). The sphere is assumed to include the ion and its nearest neighbors but to exclude the smeared out charge of eq 13 and 14; thus, it will be referred to as the exclusion sphere. The Poisson equation will then be solved explicitly for this idealized ion in the appropriate portion of the admicelle. To introduce, however, a spherical particle of finite size and charge into some portion of the admicelle will introduce a radial dependence in the field throughout the structure and into the diffuse layer. This would require the simultaneous solution of six linear and one nonlinear (The Poisson–Boltzmann equation) partial differential equations in spherical coordinates with complicated boundary conditions. Because the Poisson–Boltzmann equation is nonlinear, this system would have to be solved numerically. It is not at all clear that such an approach can be justified in light of the level of approximation already implicit in the equations. As an approximate alternative, we will instead solve the Poisson equation only for the region of the admicelle in which the ion is found. The effects of the charges in the rest of the system on the central ion will be incorporated into the solution by requiring that the potential outside the sphere goes to the macropotential given by eq 13 and 14 as the distance from the ion goes to infinity. Another difficulty in the analysis is that by including nearest neighbors in the exclusion sphere, the size of sphere needed might be found to be larger than the thickness of the upper charge layer of the admicelle. The reason for accepting this limitation rather than using an exclusion cylinder is to avoid a solution in terms of Fourier–Bessel integrals, since it is desired that the final adsorption isotherm be useful computationally and also be reasonably tractable. The charges on the nearest-neighbor ions will be neglected initially; their contribution to the electrical potential of the central ion will be added in later, a procedure justified by the linear superposition theorem.

We begin the analysis of the potential experienced by a charge in an exclusion sphere in the upper charge layer of the admicelle. The variables and coordinate system are evident from Figure 2.

Figure 2. Simulated ion immersed in charged dielective of admicelle head region. Pseudoion is centered at $z^* = 0$, $r^* = 0$.

The potential inside and outside the sphere is given by the Poisson equation

$$r^* > a, \quad \nabla^2 \psi_T = -\frac{\epsilon_T}{\beta \epsilon_T} \tag{22}$$

$$0 < r^* < a, \quad \nabla^2 \psi_S = -\frac{e}{\epsilon_S} \delta(r^*) \tag{23}$$

where $\delta(r^*)$ is a Dirac ∇ function and a is the radius of the exclusion sphere. The boundary conditions for the problem are

$$r^* = a \qquad \psi_T = \psi_S$$

$$\frac{\partial \psi_T}{\partial r^*} = \frac{\partial \psi_S}{\partial t^*}$$

$$\lim_{r^* \to \infty} \psi_T \to \hat{\psi}_T$$

$$\lim_{r^* \to 0} \psi_S \to \frac{e}{4\pi\epsilon_S r^*}$$

where $\hat{\psi}_T$ is the macropotential given by eq 13. The condition as $r^* \to 0$ is Coulomb's law. Note the assumption that $\epsilon_T = \epsilon_S$; the dielectric constants inside and outside the exclusion sphere are assumed equal.

The solution to this mathematical problem is obtained by straightforward techniques[40] and reveals that the average potential, ψ_T^*, of an ion of finite size residing in the upper zone of the admicelle which contains both charged surfactant head groups and associated counterions (Figure 1) is given by the relatively simple expression

$$\psi_T^* = \psi_D^* + \sigma_T\left(\frac{3}{8}\frac{\alpha a}{\epsilon_T} - \frac{a}{20\alpha\epsilon_T}\right) + \sigma_B\left(\frac{\alpha a}{2\epsilon_T}\right) + \sigma_S\left(\frac{\alpha a}{2\epsilon_T}\right) \tag{24}$$

Similarly, the average potential experienced by an ion in the bottom charged zone of the admicelle is given by

$$\psi_B^* = \psi_D^* + \sigma_T\left(\frac{a}{2\epsilon_T}\right) +$$

$$\sigma_S\left(\frac{11\alpha a}{8\epsilon_T} + \frac{2l}{\epsilon_I} - \frac{a}{20\alpha\epsilon_T}\right) + \sigma_S\left(\frac{2l}{\epsilon_I} + \frac{3}{2}\frac{\alpha a}{\epsilon_T}\right) \tag{25}$$

where α is the ratio of the thickness of the charge layer (assumed to be equal for the top and bottom) to the radius of the exclusion sphere (see Figure 2). This term is given by the expression

$$\alpha = \beta/a$$

We next deal with the charge layer at the admicelle/mineral oxide interface due to adsorbed potential deter-

mining ions. At this stage in the development of the model, it is an acceptable approximation to use the potential given by the equations in Figure 1. Solving for the potential at $z = 0$, we obtain

$$\psi_W^* = \psi_D^* + \sigma_S\left(\frac{2\beta}{\epsilon_T} + \frac{2l}{\epsilon_C} + \frac{\delta}{\epsilon_W}\right) + \sigma_B\left(\frac{3\beta}{\epsilon_T} + \frac{2l}{\epsilon_C}\right) + \sigma_T\left(\frac{\beta}{2\epsilon_T}\right) \quad (26)$$

This nearly completes our analysis of the electrical work of bringing an ion into a surfactant aggregate at the mineral oxide surface. The remaining term is the potential from nearest-neighbor Coulombic interactions for ions in the admicelle.

To investigate the potential of an ion in the admicelle from Coulombic interactions with its nearest neighbors, we will assign a microstructure of surfactant and counterions within the smeared charged regions. This will also enable us to identify the number and types of "sites" into which the counterions can adsorb. Ideally we would examine all the possible configurations at each patch and for each surfactant and salt concentration, allowing the admicelle to adjust itself in such a way as to achieve the most probable configuration. This configuration would be dependent on the particular molecules involved, and each system would have to be considered separately. In this paper, we will consider the surfactant to be a sulfonate and the counterion to be sodium because this choice corresponds to the system studied experimentally. Other systems may take on different configurations than that considered here.

One reasonable structure is of a hexagonal array of head groups, their centers lying in a plane parallel to the surface of the mineral oxide. This structure is similar to one proposed by Stigter[32] in his studies of ionic micelles. Stigter assumed counterions adsorb into the hexagonal array of "holes" between the head groups. Using the packing density estimated by Scamehorn et al.[5] and assuming bilayer formation with equal packing densities in each layer of the admicelle, we arrive at a figure of 2.2. sulfonates/nm^2. For hexagonal packing this gives a distance of 0.71 nm between head-group centers. If we assume adsorbed counterions to be unhydrated, a sodium ion has a diameter of only 0.09 nm, and such an array appears possible. Evidence, however, indicates sodium ions are hydrated in aqueous solution, with a hydration number of approximately four.[41] If sodium adsorbs on the admicelle in an unhydrated state, we must account for the energy of dehydration, which is far from negligible.[41] There is also infrared (IR) evidence[42] to indicate that sodium adsorbed on sodium sulfonate micelles is fully hydrated. By use of 0.09 nm for the radius of the sodium ion and 0.14 nm for the radius of a water molecule, the *hydrated* radius of the sodium ion is 0.37 nm, so that the distance of closest approach of the centers is 0.74 nm; this distance is greater than the distance between the centers of the sodium sites in the array being discussed (0.71 nm).

If we insist that the sulfonate groups are in a hexagonal-planar array with these hydrated sodiums adsorbing in hexagonal array in the interstices, the maximum counterion binding is only 50% because of the steric restrictions. This is unacceptably low. Counterion binding for sodium sulfonate micelles is generally near 50%, and the admicelle we have postulated has a higher charge density and hence larger bindings.

If we do not require the centers of the sulfonates to be in a plane (compare Lindeman and Wennerstrom[42] and
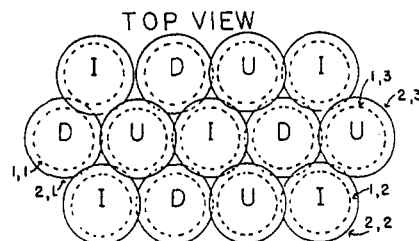

Figure 3. Top view of admicelle structure assumed for model with 100% counterion binding. up sites indicated by U, "down" sites by D, intermediate sites by I. Dotted circles represent sulfonate ions; solid circles represent hydrated counterions.
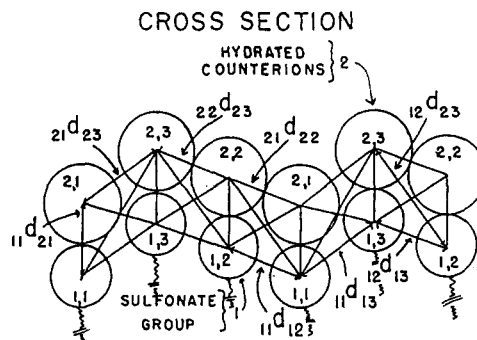

Figure 4. Cross section of model array showing intermolecular distances. The distance between the up sulfonate and the down sulfonate centers is $_{11}d_{13}$, between the up sodium and "intermediate" sulfonate is $_{12}d_{23}$.

Hirasaki and Lawson[43]), it is possible to construct an array with a maximum obtainable binding of 100%. Lindeman and Wennerstrom[42] state that IR studies on sodium sulfonate micelles suggest that the hydrated counterions are positioned between the three oxygens of the sulfonate ion. They also cite evidence indicating water does not penetrate into the hydrocarbon core of sodium sulfonate micelles. This leads to a picture of the surfactant ions moving up and down in tubes that are in a hexagonal array, the ions being fairly well restricted to the centers of the tubes (Figures 3 and 4).

This picture makes the reasonable assumption that there is an average correlation between the relative motions of nearest neighbors so that no surfactant hydrocarbon moiety is ever exposed to either the aqueous phase or to a hydrated counterion; for this to happen, the center of the sulfonate must rarely move more than ±0.21 nm from its average position (Figure 4). If the oxygen "cup" on each sulfonate is then assumed to be a potential "adsorption site" for the hydrated counterions, there are three types of counterion adsorption sites: up, down, and intermediate. The potential of a surfactant ion or an adsorbed counterion due to nearest-neighbor Coulombic interactions can then be estimated if the contribution of each site is multiplied by a fractional occupation. Of course, we are not picturing an adsorbed ion as actually occupying a particular site but rather as spending appropriate fractions of its time in the admicelle in local environments in which its Coulombic interactions with its nearest neighbors are approximately that of an ion in one of the three adsorption sites in Figure 4.

The detailed study necessary to rigorously differentiate between the various possible surfactant/counterion configurations would be unjustifiable at the present stage of surfactant adsorption studies. There is no data at all on such fundamental parameters as counterion binding or aggregation numbers; nor are there any IR or NMR studies to provide clues concerning details of the admicelle structure. When combined, however, with the IR evidence

cited by Lindeman and Wennerstrom[42] and the intuitively appealing possibility of 100% counterion binding, the choice of the admicelle structure shown in Figures 3 and 4 for calculating the contribution of nearest-neighbor interactions to counter surfactant adsorption potential seems reasonable until further studies are carried out.

Having now chosen a local structure for the admicelle, it is possible to write the electrical potential of the ions from nearest-neighbor Coulombic interactions. Note that the average contribution of a particular type of site to the potential of the other sites is directly proportional to the fractional occupancy of that site. We will derive the expressions for the nearest-neighbor contributions to the adsorption potential of one sulfonate then simply present the potentials for the remaining five sites.

Consider a sulfonate ion in the down position. It has six nearest-neighbor sulfonates and seven partially occupied nearest-neighbor hydrated sodium sites (Figure 4). Of the sulfonate neighbors, three are in the up and three in the intermediate position. Of the sodiums, some fraction between 0 and 1 are in the down, intermediate, and upper positions. The Coulombic potential of the sulfonate ion in the down position due to its nearest neighbors is then given by the following expression

$$\psi_{S^-,N,D} = \frac{e}{4\pi\epsilon_0}\left[\left(\frac{3}{_{11}d_{12}} + \frac{3}{_{11}d_{13}}\right) - \left(\frac{1}{_{11}d_{21}}\frac{\sigma_{Na^+,D}}{\sigma_m/3} + \frac{\sigma_{Na^+,I}}{\sigma_m/3}\frac{3}{_{11}d_{22}} + \frac{\sigma_{Na^+,U}}{\sigma_m/3}\frac{3}{_{11}d_{23}}\right)\right] \quad (27)$$

where e is the elementary electrical quantum, ϵ_0 is the dielectric constant of free space, $_{11}d_{12}$ is the distance between the center of a sulfonate ion in the down position and a sulfonate ion in the intermediate position (see Figure 4), $_{11}d_{21}$ is the distance between the centers of the sulfonate in the down position and a hydrated sodium ion in the down position, σ_m is the density of sulfonate in a layer of the admicelle (ions/nm²) assumed to be one-half of the bilayer adsorption density, $\sigma_{Na^+,I}$ is the average density of hydrated sodium counterions adsorbed in the intermediate position in ions/nm², and the remaining terms are defined analogously. Note that, for example,

$$0 \leq \frac{\sigma_{Na^+,I}}{\sigma_m/3} \leq 1$$

It is readily apparent that equations similar to eq 27 can be written for $\psi_{S^-,N,I}$ and $\psi_{S^-,N,U}$. Furthermore, because $\sigma_{Na^+,I}$ and $\sigma_{Na^+,U}$ may differe in the top layer and bottom layer, there are actually six potentials of interest: $\psi_{S^-,N,D,T}$, $\psi_{S^-,N,I,T}$, $\psi_{S^-,N,U,T}$, $\psi_{S^-,N,D,B}$, $\psi_{S^-,N,I,B}$, and $\psi_{S^-,N,U,B}$, where the subscripts T and B denote top and bottom layers, respectively.

The micropotential of a sodium ion due to nearest-neighbor interactions can also be written. It is not difficult to now obtain the following expression:

$$\psi_{Na^+,N,U} = \frac{e}{4\pi\epsilon_0}\left[\left(\frac{\sigma_{Na^+,I}}{\sigma_m/3}\frac{3}{_{23}d_{22}} + \frac{3}{_{23}d_{21}}\right)\frac{\sigma_{Na^+,D}}{\sigma_m/3} - \left(\frac{3}{_{23}d_{11}} + \frac{3}{_{23}d_{12}} + \frac{1}{_{23}d_{13}}\right)\frac{\sigma_{Na^+,U}}{\sigma_m/3}\right] \quad (28)$$

Furthermore, there are, as with the surfactants, six such micropotentials: $\psi_{Na^+,N,U,T}$, $\psi_{Na^+,N,I,T}$, $\psi_{Na^+,N,D,T}$, $\psi_{Na^+,N,U,B}$, $\psi_{Na^+,N,I,B}$, and $\psi_{Na^+,N,D,B}$.

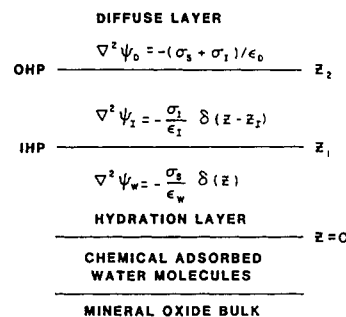The electrical potential of an adsorbed surfactant ion in an admicelle from nearest-neighbor Coulombic inter-

Figure 5. Double-layer geometry below surface concentration at which admicelles form.

actions is assumed to be an average of the potentials in the various sulfonate sites, assumed to be fully occupied

$$\hat{\phi}_{S^-,N} = (1/3)(\phi_{S^-,N,U} + \phi_{S^-,N,D} + \phi_{S^-,N,I}) \quad (29)$$

where $\phi_{S^-,N,D}$ is the reduced Coulombic potential from nearest-neighbor interactions of a sulfonate in the down position, given by the expression

$$\phi_{S^-,N,U,T} = (e/kT)\psi_{S^-,N,U,T} \quad (30)$$

The circumflex in the term $\hat{\phi}_{S^-,N}$ indicates that it is an average quantity.

We will also present expressions for the total charge on the admicelle based on the assumptions of this model. The total number densities of sodium ions adsorbed in the top and bottom layers of the admicelle are given by

$$\sigma_{Na^+,T} = \sigma_{Na^+,D,T} + \sigma_{Na^+,I,T} + \sigma_{Na^+,U,T} \quad (31)$$

$$\sigma_{Na^+,B} = \sigma_{Na^+,D,B} + \sigma_{Na^+,I,B} + \sigma_{Na^+,U,B} \quad (32)$$

The total charge on the top and bottom layers of the admicelle is given by

$$\sigma_T = (\sigma_{Na^+,T} - \sigma_m) \quad (33)$$

$$\sigma_B = (\sigma_{Na^+,B} - \sigma_m) \quad (34)$$

The charge density due to the adsorbed counterions, σ_{Na^+}, and that due to the surfactants in the admicelle, σ_m, are, of course, simply related to the adsorption densities on the local patch in question Γ_{Na^+} and Γ_{S^-}, respectively, occurring in eq 6.

This completes our analysis of the electrical contributions to admicelle formation. Yet we still do not have a complete set of equations for determining the CAC of a local patch given the charge density on that patch after admicelle formation. The reason is the counterion binding. The equations for the electrical potential include as variables the occupancy of the various counterion adsorption sites in the admicelle, e.g., $\sigma_{Na^+,D}/(\sigma_m/3)$, but we do not have expressions for the chemical potentials of the counterions in the various sites—recall that there are six types of sites in the proposed structure, three for each layer. This situation is very similar to that encountered in the pseudophase separation model for micelles. An empirical factor is required to properly adjust the counterion binding.

In region I for ions adsorbed on a local patch that has not undergone a phase transition to local bilayer coverage, we will neglect discreteness corrections and use for the potential the solution the equations shown in Figure 5. The potential-determining ions are located in the plane $Z = 0$, which corresponds to the metal oxide hydration layer. The IHP is assumed to be the plane of the distance of closest approach of all adsorbed ions and these ions are all also assumed to have their motion restricted to that plane. The arrangement is depicted schematically in Figure 6.
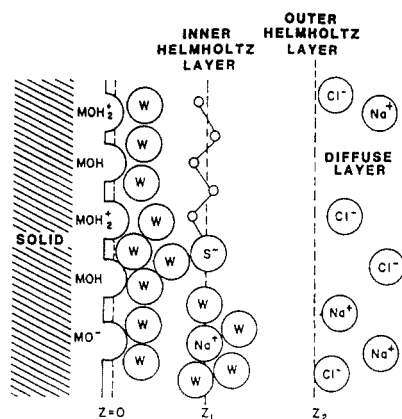
Figure 6. Schematic representation of an oxide interface showing possible locations for molecules including surfactant, counterions, co-ions, and water.

The outer Helmholtz plane (OHP) is taken as the beginning of the diffuse part of the double layer, where the ion population distribution can be described by the Poisson–Boltzmann equation. The equations describing the system in terms of the charge density at the potential determining layer (σ_S) and the charge at the IHP are easily solved to give

$$\phi_D = \cosh^{-1}\left[1 + \frac{(\sigma_S + \sigma_I)^2}{4kT\pi\rho_0\epsilon_D}\right] \quad (35)$$

$$\phi_I - \phi_D = \frac{z_3 - z_2}{\epsilon_I}(\sigma_S + \sigma_I) \quad (36)$$

$$\phi_W - \phi_I = \frac{z_2 - z_1}{\epsilon_W}\sigma_S \quad (37)$$

At this point, we wish to reiterate our belief that those parameters now used to characterize the surface charge based on the complexation site binding model will also apply to surfactant adsorption provided the hydrophobic effect is taken into account. Presentation of the details of our approach is well beyond the scope of the present paper, but we should note that a recent presentation by Zelenka and Radke[9] proceeds generally along the lines that we envision when region I is considered. Admicellar formation will have to be taken into account, however, to obtain a complete picture of the electrical state of a surface in the presence of surfactants.

Adsorption Isotherms

Expressions for the electrical potentials of both surfactant (sulfonate) ions and (sodium) counterions in admicelles have been obtained so that the electrical contribution to the $(\bar{W}_i - W_i)$ term appearing in eq 6 is known. For simple ions such as sodium, we will assume this to be the sole contribution to the work term, while for surfactants, an additional contribution proportional to the length of the surfactant's hydrocarbon tail is added. For a surfactant molecule in the admicelle, eq 6 takes the following form:

$$\left(\hat{\phi}_{S^-} + \frac{m\omega}{kT}\right) - \ln\left(\frac{4\pi^2\sigma_m}{\rho_{S^-}\Lambda_{S^-}}\right) = 0 \quad (38)$$

Here we assume that $\bar{q}_{S^-} = q_{S^-}$. Note that $\check{\phi}_{S^-}$ is the ensemble average reduced micropotential of a surfactant molecule in either the top or the bottom layer of the admicelle structure. The potential in both layers must necessarily be equivalent to maintain equal chemical po-

tentials in the layers. Thus,

$$\hat{\phi}_{S^-} = \hat{\phi}_{S^-,T} = \hat{\phi}_{S^-,B} \quad (39)$$

Equation 6 also applies to counterions, thus for the top layer

$$\hat{\phi}_{Na^+,T} - \ln\left(\frac{\sigma_{Na^+,T}}{\rho_{Na^+}\Lambda_{Na^+}}\right) = 0 \quad (40)$$

A similar expression for the bottom layer can be written as follows:

$$\hat{\phi}_{Na^+,B} - \ln\left(\frac{\sigma_{Na^+,B}}{\rho_{Na^+}\Lambda_{Na^+}}\right) = 0 \quad (41)$$

Since the bulk concentration of sodium ions is the same in eq 40 and 41, a relationship between the micropotentials of a sodium ion in each of the layer exists. This relationship must be satisfied to maintain the sodium chemical potential the same in both layers.

To summarize the potentials in a convenient form, we write the following:

$$\phi^*_{S^-,T} = \phi_T - \left(\frac{e^2}{kT}\right)\left(\frac{a}{20\alpha\epsilon_T}\right)\sigma_T + \hat{\phi}_{S^-,N,T} \quad (42)$$

$$\phi^*_{S^-,B} = \phi_B - \left(\frac{e^2}{kT}\right)\left(\frac{a}{20\alpha\epsilon_B}\right)\sigma_B + \hat{\phi}_{S^-,N,B} \quad (43)$$

$$\phi_T = \phi_D + \left(\frac{e^2}{kT}\right)\left(\frac{\beta}{2\epsilon_T}\right)\sigma_S + \left(\frac{e^2}{kT}\right)\left(\frac{\beta}{2\epsilon_T}\right)\sigma_B + \left(\frac{e^2}{kT}\right)\left(\frac{3\beta}{8\epsilon_T}\right)\sigma_T \quad (44)$$

$$\phi_B = \phi_D + \left(\frac{e^2}{kT}\right)\left(\frac{3\beta}{2\epsilon_B} + \frac{2l}{\epsilon_C}\right)\sigma_S + \left(\frac{e^2}{kT}\right)\left(\frac{11\beta}{8\epsilon_B} + \frac{2l}{\epsilon_c}\right)\sigma_B + \left(\frac{e^2}{kT}\right)\left(\frac{\beta}{2\epsilon_T}\right)\sigma_T \quad (45)$$

$$\phi_D = \cosh^{-1}\left\{1 + \left(\frac{\sigma_D + \sigma_B + \sigma_T}{4kT\rho_0\epsilon_D}\right)^2\right\} \quad (46)$$

$$\sigma_T = \sigma_{Na^+,T} - \sigma_m \quad (47)$$

$$\sigma_B = \sigma_{Na^+,B} - \sigma_m \quad (48)$$

$$\sigma_{Na^+,T} = \sigma_{Na^+,D,T} + \sigma_{Na^+,I,T} + \sigma_{Na^+,U,T} \quad (49)$$

$$\sigma_{Na^+,B} = \sigma_{Na^+,D,B} + \sigma_{Na^+,I,B} + \sigma_{Na^+,U,B} \quad (50)$$

$$\hat{\phi}_{S^-,N,T} = (1/3)(\phi_{S^-,N,T,U} + \phi_{S^-,N,T,I} + \phi_{S^-,N,T,D}) \quad (51)$$

$$\hat{\phi}_{S^-,N,B} = (1/3)(\phi_{S^-,N,B,U} + \phi_{S^-,N,B,I} + \phi_{S^-,N,B,D}) \quad (52)$$

To construct an adsorption isotherm, it is necessary to relate the surface charge density, σ_S, to that surfactant bulk concentration ρ_S (CAC) at which admicelles form on all patches of the surface having that charge. Patches having a greater surface charge are already covered with admicelles while patches having a lesser charge are not.

Let us now assume that we have the surface charge density, σ_S, and wish to calculate the CAC. The following are either known constants or adjustable parameters: m, $\bar{\omega}_A$, T, σ_m, α, β, l, ρ_{Na^+}, all the molecular spacings of the admicelle structure, and the dielectric constants applicable in the separate regions of the admicelle. The following are dependent variables: ρ_s, $\sigma_{Na^+,U,T}$, $\sigma_{Na^+,I,T}$, $\sigma_{Na^+D,T}$, $\sigma_{Na^+,U,B}$, $\sigma_{Na^+,I,B}$, $\sigma_{Na^+D,B}$. The independent equations are eq 38–41. This leaves four unknowns more than we have equations.

This problem is perhaps a difficult one and will not be specifically addressed at this time. Indeed, for the model assumed here, the potential, $\phi_{S^-,N,T}$ and $\phi_{S^-,N,B}$, results in quite small corrections to the macropotential, which is consistent with the results of polarizability theory.[39]

To determine the region I adsorption of surfactant at the IHP we note that eq 6 reduces to

$$\left(\phi_I - \frac{n\bar{\omega}_I}{kT} \right) - \ln \left(\frac{4\pi^2 \Gamma}{\rho_{S^-} \Lambda_{S^-}} \right) = 0 \qquad (53)$$

(Note: for a monovalent surfactant $e\Gamma = \sigma_S$). This equation gives the adsorption of the surfactant into the IHP. Its adsorption is enhanced by the factor $n\bar{\omega}_I$ as compared to simple ions. This enhancement will permit, for example, surfactant to almost quantitatively displace co-ions from the IHP.[45] The charge at the IHP is

$$\sigma_I = e \left(\Gamma_{Na^+} - \Gamma_I - \Gamma_{Cl^-} \right) \qquad (54)$$

Equation 53 provides the necessary expression for Γ_I for use in eq 1. To determine ϕ_I, one must evaluate σ_S, which depends on solution pH and T along with Γ_{Na^+} and Γ_{Cl^-}. These all must be solved for simultaneously since they are coupled.

Given additional facts to help establish counterion (binding) adsorption into the admicellar structure, we then have a theory for predicting surfactant adsorption in all regions of the isotherm as well as for predicting the ζ-potential as a function of surfactant solution concentration. Thus,

$$-\zeta = \psi_D^* \int_{\sigma_S^*}^{(\sigma_S)_{max}} f(\sigma_S) \, d\sigma_S + \int_{(\sigma_S)_{min}}^{\sigma_S^*} \psi_D(\sigma_S) f(\sigma_S) \, d\sigma_S \qquad (55)$$

where $\psi_D(\sigma_S)$ is the potential at the diffuse double layer (shear plane) for those portions of the surface on which admicelles have not yet formed as given by eq 35 and ψ_D^* for admicelles is determined by the total charge ($\sigma_S + \sigma_B + \sigma_T$). Calculations and measurements show that the ζ-potential can, and often does, change sign at increasing levels of surfactant adsorption. According to eq 55, the point at which this sign change occurs can be in region I or II, or it may not occur at all if plateau adsorption is reached before the surface charge is neutralized.

Finally we note that this approach also incorporated parameters characteristic of the molecular structure of the surfactant, m, σ_m, α, β, l, $\bar{\omega}_A$, $\bar{\omega}_I$, n, and all of the structure parameters for the admicelle are functions of the surfactant structure.

We recognize that the development presented here incorporates approximations not yet justified by experiments and that some of the mathematical steps can be performed with greater precision (and with correspondingly increased labor and complexity in the final expression); yet this new approach unifies many aspects of surfactant adsorption not heretofore considered in any other theory.

Simplified Adsorption Isotherm. To facilitate a tractable solution, we shall ignore eq 40 and 41, which relate to the distribution of counterions between the solution and the top and bottom layers of the admicelle. With this assumption, it can be shown that eq 38 can then be written in the form

$$\rho_{S^-} = \frac{D \exp(C - B\sigma_s)}{y + (y^2 - 1)^{1/2}} \qquad (56)$$

where

$$y = 1 + \frac{(\sigma_S + A)^2}{E\rho_0}$$

$$\rho_0 = \rho_{S^-} + \rho_{Na^+}$$

$$A = \sigma_T + \sigma_B$$

$$B = \frac{e^2}{2kT} \left(\frac{\beta}{2\epsilon_T} + \frac{3\beta}{2\epsilon_B} + \frac{2l}{\epsilon_C} \right)$$

$$C = \frac{e^2}{2kT} \left[\left(\frac{a}{20\alpha\epsilon_T} - \frac{\beta}{2\epsilon_T} - \frac{11\beta}{8\epsilon_B} - \frac{2l}{\epsilon_c} \right) \sigma_B + \left(\frac{a}{20\alpha\epsilon_B} - \frac{3\beta}{8\epsilon_T} - \frac{\beta}{2\epsilon_B} \right) \sigma_T \right] - \frac{1}{2} (\hat{\phi}_{S^-,N,T} + \hat{\phi}_{S^-,N,B})$$

$$D = \frac{4\pi^2 \sigma_m \exp\left(\dfrac{m\bar{\omega}_A}{kT} \right)}{\Lambda_{S^-}}$$

$$E = 4kT\epsilon_0$$

Because eq 39 is not necessarily satisfied due to preferential adsorption of counterions into the top and bottom layers of the admicelle, we have in deriving 56 used the approximation

$$\hat{\phi}_{S^-} = (1/2)(\phi_{S^-,T} + \phi_{S^-,B}) \qquad (57)$$

The quantities A, B, C, and E are constants. We would not expect A or E to change for different surfactants in a homologous series. B and C will differ as the surfactant's chain length is increased. These predictions can be tested experimentally.

Results

To the authors' knowledge, an independent method for measuring the distribution of surface charge densities does not now exist. The approach here is as follows: (1) The best estimates were chosen for the parameters characteristic of the molecular structure of the surfactant, m, σ_m, a, α, β, l, and $\bar{\omega}_A$. (2) The parameters σ_T, σ_B, ϵ_T, ϵ_B, ϵ_C, and ϵ_D originate from the electrostatics of the system. Reasonable estimates of ϵ_C and ϵ_D are easily chosen since these should vary little from their bulk values. The parameters σ_T, σ_B, ϵ_T, and ϵ_B will be adjustable. (3) The range of $F_A(\sigma_S^*)$ was determined for each surfactant in the homologous series by using experimentally obtained isotherms and bilayer coverage in conjunction with eq 2. The range of $F_A(\sigma_S^*)$ to be used for calculations was chosen to correspond to the surfactant with the smallest range. Thus, the adjustable parameters are fit over a range of $F_A(\sigma_S^*)$ that lies within the $F_A(\sigma_S^*)$ of all the surfactants. (4) To solve for the parameters σ_T, σ_B, ϵ_T, and ϵ_B, the generalized reduced gradient method[47-50] was used, which minimizes a nonlinear objective function subject to nonlinear constraints. The objective function is based on the sum of the squares of the errors of the σ_S^*'s of the different surfactants

$$SSE = \sum_{i=1}^{np} \left[\sum_{j=2}^{ns} \frac{\sigma_S^*{}_i - \sigma_S^*{}_{i,j}}{\sigma_S^*{}_i} \right] \qquad (58)$$

(47) Lasdon, L. S.; Warren, A. D.; Jain, A.; Ratner, M. "Design and Testing of a Generalized Reduced Gradient Code for Nonlinear Programming", ACM Transactions on Mathematical Software, 1978; Vol. 4, No. 1, pp 34–50.
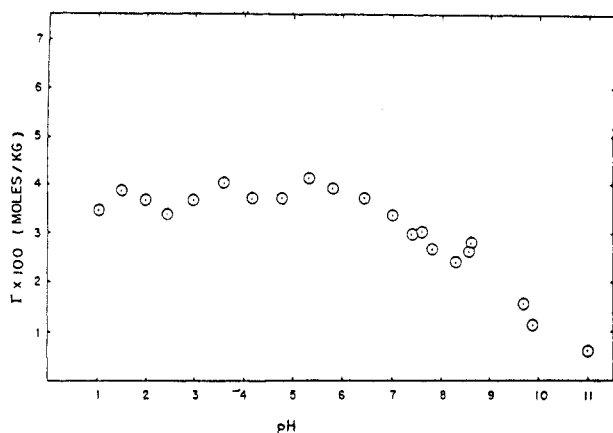
(48) Lasdon, L. S.; Warren, A. D. "Design and Implementation of Optimization Software"; Greenberg, H., Ed.; Sijthoff and Noordhoff, 1969.

(49) Abadie, J.; Carpentier, J. "Optimization"; Fletcher, R., Ed.; Academic Press: London, 1969.

(50) Himmelblau, D. M. "Applied Nonlinear Programming"; McGraw-Hill: New York, 1972.
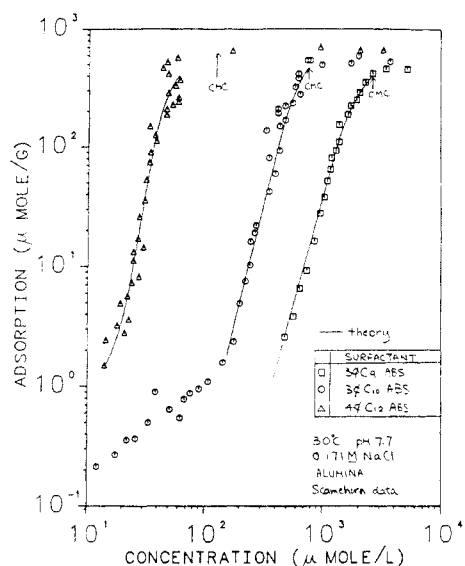
Figure 7. Effect of alkyl chain length on adsorption of ABS isomers on alumina.

Figure 8. Plateau adsorption as a function of pH for $3\phi C_9 ABS$ on α-alumina.

**Table I. Constants and Molecular Parameters Used To Fit Data**

$\bar{\omega}_A$	-0.92 kcal/mol
σ_m	2.29 charges/nm^2
a	1.85 nm
β	2.00 nm
α	1.08
ϵ_C	2.20
ϵ_D	78.0

	$3\phi C_9$	$3\phi C_{10}$	$4\phi C_{12}$
l, nm	1.28	1.34	1.40
m	12.5	13.5	14.5
MW, g/mol	306.3	320.4	348.3

where np represents the number of data points and ns denotes the number of surfactants in the homologous series. The index j starts at 2 since one of the surfactants is chosen as the test surfactant. The constraints are eq 56 which must be satisfied for each data point (which connects σ_S to the data) and

$$\sigma_k = \frac{\Delta\psi}{\beta}(\epsilon_k + 6) \tag{59}$$

where

$$\epsilon_k = \frac{\epsilon_{bulk} - 6}{1 + (1.2 \times 10^{-17})(\Delta\psi/\beta)^2} \tag{60}$$
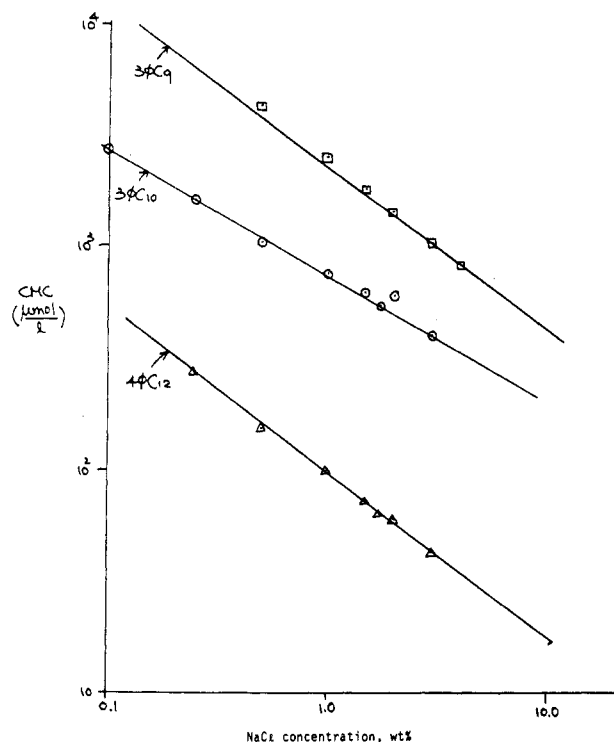
Figure 9. Pure component cmc data used to obtain phase separation model constants for monomer/micelle equilibrium for $3\phi C_9 ABS$, $3\phi C_{10} ABS$, and $4\phi C_{12} ABS$.
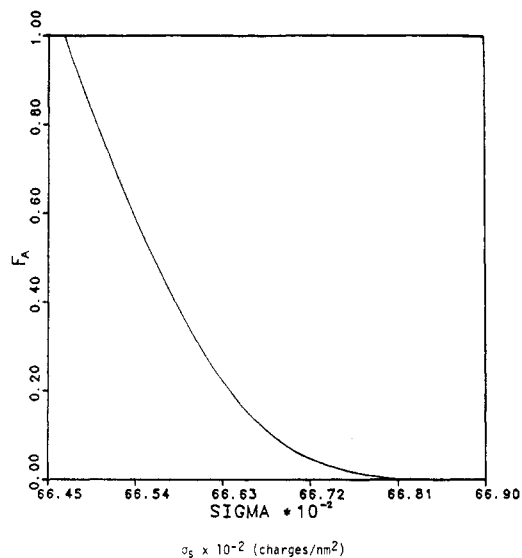

$\sigma_S \times 10^{-2}$ (charges/nm^2)

Figure 10. Cumulative distribution function used to fit isotherms in this study. Note that $F_A(\sigma_S)$ is the fraction of the surface having a charge density of σ_S or greater.

Table II. Values of Adjustable Parameters

σ_T	-0.031 charges/nm^2
σ_B	-0.679 charges/nm^2
ϵ_T	77.96
ϵ_B	36.69

which connects σ_k and ϵ_k (ref 51) where k represents either T or B, the top and bottom of the admicelle, respectively.

To test the applicability of the theory the model was used on the data of Scamehorn et al.[5] The final results appear in Figure 7. Data used to determine bilayer coverage appear in Figure 8, cmc data in Figure 9. The cumulative charge distribution appears in Figure 10. This function is defined so that $F_A(\sigma_S^*)$ is the fraction of the
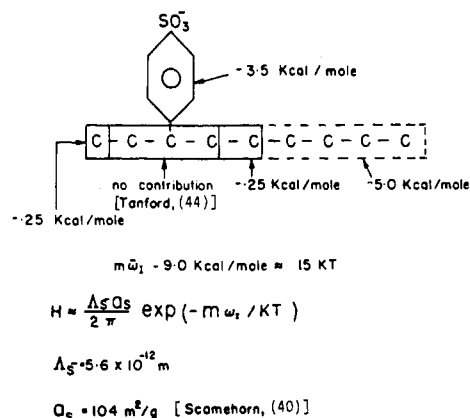
Figure 11. Contributions to Henry's law adsorption of hydrophobic moieties of $3\phi C_{10}ABS$.

surface charge density greater than or equal to σ_S. Table I lists the constants and molecular parameters used to fit the data in Figure 7, and Table II shows the values determined for the adjustable parameters.

Discussion of Results

The pseudophase separation model for micellization requires that the surfactant chemical potential remain constant for monoisomeric surfactant concentrations in excess of the cmc. On the basis of this concept, we would expect adsorption to reach a plateau at the cmc even if complete bilayer coverage has not yet been achieved. The cmc values shown in Figure 9 were obtained on the basis of surface tension measurements, and these values are indicated in Figure 7. It is seen that adsorption does not cease abruptly at the CMC but reaches a constant value at somewhat higher solution concentrations. This discrepancy is due entirely to the small increase in surfactant chemical potential which results from the progressive formation of larger surfactant agregates. Thus, the pseudophase separation model is, we should remember, an approximation albeit an excellent one.

Region II Adsorption. Even though we have applied the simplified model to experimental data, we still encounter the weakest link remaining in the modeling of surfactant adsorption: the absence of an independent expression for the surface charge density. The mean of this distribution is potentially accessible through a combination of counterion activity, ζ-potential, and adsorption density measurements. The mean surface charge density of 66.58×10^{-2} charge/nm^2 obtained using the Scamehorn[5] data, considering the solution pH was 7.7 and that the point of zero charge of γ-alumina is 9.1, would appear to be a reasonable value. The distribution is a sharp one since as shown in Figure 10 the charge density varies only from 66.47×10^{-2} to 66.86×10^{-2} charge/nm^2. This indicates a relatively homogeneous surface and accounts for the steep slopes of the isotherms in region II (see Figure 7). It seems evident that surfactant adsorption does have potential to be a molecular probe for aqueous–solid surfaces.

The values of the adjustable parameters in Table II fall into physically reasonable ranges. The values of σ_T and σ_B show that the formation of the bilayer slightly overbalances the charge on the surface. The value of σ_T is smaller than σ_B since not as many counterions are needed in the bottom layer with the surface charge balancing some of the surfactant ions. The effective dielectric constant ϵ_T and ϵ_B lie within the acceptable range of 6–78 by James and Healy.[51] Also $\epsilon_T > \epsilon_B$, which is predicted by eq 59.

With the success of the adjustable parameters it would indicate that the constants and estimated molecular parameters in Table I represent reasonable values.

Since there are a large number (four) of adjustable parameters in addition to the distribution function which enter into the theory, it is only possible on the basis of the limited available experimental data presented here to conclude that the model does appear to have merit and that further, more detailed studies are warranted to test the model.

Region I Adsorption. The experimental isotherm satisfied Henry'law and the values of Henry's constant that best fits each isotherm are given in Table III. Equation 53 applies and this expression can be rearranged to give

$$\Gamma_I = \frac{\rho_S \cdot \Lambda_{S,I}}{4\pi^2}[y + (y^2 - 1)^{1/2}] \exp\left[\frac{-n\bar{\omega}_I}{kT} + \frac{\sigma_S + \sigma_I}{c_0}\left(\frac{kT}{e}\right)\right]$$
(61)

where

$$C_0 = \frac{\epsilon_I}{z_3 - z_2}$$

Since σ_S is small (66.58×10^{-2}) and the capacitance of the OHP is, for some cases, about 10 $\mu F/cm^2$,[9] then

$$\frac{\sigma_S + \sigma_I}{C_0}\frac{kT}{e} \ll \frac{-n\bar{\omega}_I}{kT}$$

Furthermore for small values of adsorption

$$y = 1 + \frac{(\sigma_S + \sigma_I)^2}{4kT\epsilon_D\rho_0} = 10.56$$

σ_I is neglected in this calculation since it will only serve to reduce y (σ_I will have sign opposite of σ_S) and

$$\rho_0 \equiv \rho_{Na^+} \; \rho_{S^-} \cong \rho_{Na^+}$$

With these approximations

$$\Gamma_I \cong 0.534\rho_S \cdot \Lambda_{S^-} \exp\left(-\frac{n\bar{\omega}_I}{kT}\right)$$
(62)

which is Henry's law since now Γ_I varies linearly with ρ_S.

We can now compare predicted results using experimentally determined parameters. It has been postulated[40] that the hydrocarbon chain of the surfactant interacts with the substrate. However, due to steric constraints, the first few methyl groups next to the charged head group are excluded from this interaction. Using the values of H in Table III and $\bar{\omega}_I = -0.73$ kcal/mol as reported by Scamehorn et al.[5] we can calculate n by eq 58. The resulting values are 10.4, 8.7, and 7.3 for $4\phi C_{12}$, $3\phi C_{10}$, and $3\phi C_9$, respectively. The fact that these results are smaller than their corresponding m values listed in Table I should not be interpreted as a confirmation of the theory, but rather as an encouraging trend. Complete confirmation will require a systematic study of a large number of factors all measured simultaneously. Such a systematic study has not yet been reported.

There have been conflicting experimental findings reported for region I isotherms, but these are reconciled by eq 61. Scamehorn et al.[5] and the results reported here show that the Henry constant increases with increasing tail length. Wakamutsu and Fuerstenau[9] also found Henry's law to apply in region I but did not find any

(51) James, R. O.; Healy, T. W. *J. Colloid Interface Sci.* 1972, *40*, 42.

Table III. Values of Henry's Constant

$H_{4PhC_{12}}$	9.01×10^{-2} L/g
$H_{3PhC_{10}}$	1.24×10^{-2} L/g
H_{3PhC_9}	2.27×10^{-3} L/g

dependence on tail length. Nunn[45] found Henry's law in the presence of added electrolyte, but when no additional electrolyte was added, the isotherms exhibited a decreasing slope throughout region I.

Since Wakamatsu and Fuerstenau performed their experiments at pH 7 compared to pH 8, here, in their study larger values of the surface charge are possible. Hence

$$\frac{\sigma_S + \sigma_I}{C_3} \gg -\frac{m\bar{\omega}_I}{kT}$$

In this case, increasing the tail length will not change the Henry constant—a trend they reported.

Finally, in the presence of little or no added salt, eq 57 takes the form

$$\Gamma_I = \left(\frac{\rho_{S^-}}{\rho_{S^-} + \rho_{Na^+}}\right) \frac{\Lambda_{S^-}}{2\pi^2} \frac{(\sigma_S + \sigma_I)^2}{4kT\epsilon_D} \exp\left(-\frac{n\bar{\omega}_I}{kT} + \frac{\sigma_c + \sigma_I}{c_0}\right)$$

(63)

In this limit, Γ_I is not linearly related to ρ_S and a decreasing slope with increasing ρ_{S^-} will be observed. This corresponds to the findings reported by Nunn.[45]

Letters

Site Specificity in the Room Temperature Deuterium Exchange of Cyclopentane over Pt/CPG Catalysts

Robert L. Augustine* and Russell Wesdyk

Department of Chemistry, Seton Hall University, South Orange, New Jersey 07079

Several single-turnover (STO) characterized Pt/CPG catalysts were used for the H/D exchange on cyclopentane. The data obtained indicated that polydeuterium exchange, which occurred by way of a multiple α,β-exchange process, took place on those sites responsible for direct alkene hydrogenation in the STO procedure. Monodeuterated products, which are formed by an α-substitution process, are produced by reactions on those surface sites that are not involved in alkene hydrogenation or isomerization. Mechanistic considerations indicate that the α,β-exchange sites are more coordinately unsaturated than are those on which α-exchange occurs.

The catalytic H/D exchange on alkanes has been rather extensively studied as a means of determining the nature of the interaction between hydrocarbons and catalyst surfaces.[1] While the results obtained have provided a considerable amount of information concerning this process, they were not always readily interpretable on the basis of a single type of metal/hydrocarbon interaction. Instead, it has been proposed that at least two different types of sites are present on the catalyst surface.[2] It has been suggested that on one of these simple monodeuterium exchange takes place through an α-exchange process while another type of site produces polydeuterated products through a series of α,β exchanges taking place by way of a sequence of 1,2-diadsorbed intermediates. This difference can most easily be seen by reference to Scheme I in

Table I. Pt/CPG Catalyst Characterization Data[a]

	% surface sites[b]				
catalyst	1[c]	2[c]	3[c]	4[d]	5[c]
type I	72	64	60	32	28
type II	7	11	12	22	23
type III	21	25	28	46	49
types II and III	28	36	40	68	72
dispersion	0.88	0.66	0.49	0.44	0.61

[a] Obtained by using the single-turnover procedure described in detail in ref 5. [b] Type III sites promote direct alkene hydrogenation, type II are alkene isomerization sites, and type I sites only absorb hydrogen. These types of sites previously have been tentatively labeled[5] ^3M, ^2M, and M^6 sites, respectively. [c] 6.9% Pt/CPG. [d] 6.1% Pt/CPG.

which the generally accepted general mechanism for deuterium exchange[1] is depicted. Surface sites that have a high degree of coordinative unsaturation such as corners or kinks should more readily accommodate the diadsorbed species formed in step 3. Alternate reversal of this step with deuterium incorporation (step 3) and reformation of the 1,2-diadsorbed species with the breaking of other C–H

(1) Burwell, R. L., Jr. *Acc. Chem. Res.* **1969**, *2*, 289; *Catal. Rev.* **1972**, *7*, 25. Kemball, C. *Catal. Rev.* **1971**, *5*, 33.

(2) Anderson, J. R.; Kemball, C. *Proc. R. Soc. London, Ser. A* **1954**, *223*, 361. Rowlinson, H. C.; Burwell, R. L., Jr.; Tuxworth, R. H. *J. Phys. Chem.* **1955**, *59*, 225. Inoue, Y.; Herrmann, J. M.; Schmidt, H.; Burwell, R. L., Jr.; Butt, J. B.; Cohen, J. B. *J. Catal.* **1978**, *53*, 401.